Research Article Open Access

Geospatial Assessment of Land Use/Land Cover Change and Land Surface Temperature Dynamics Using Multi-Index Analysis and CA-Markov Modeling from 1990-2022 in Lahore, Pakistan

Areeba Rehman [1]*, Sana Ashraf [1], Salman Tariq [2, 3], Muhammad Waleed [4], Hira Khalid [1], Hina Mazhar [1], Nehal Islam [1], Bareera Munir [1]

[1]College of Earth and Environmental Sciences, Faculty of Geosciences, University of the Punjab, Lahore, Pakistan.
[2]Department of Space Science, Faculty of Geosciences, University of the Punjab, Lahore, Pakistan.
[3]Remote Sensing, GIS and Climatic Research Lab (National Center of GIS and Space Applications), Centre for Remote Sensing, University of the Punjab, Lahore, Pakistan.
[4]Department of Land Resources and Space Information Technology, College of Natural Resources and Environmental Sciences, North West Agriculture and Forestry University, Yangling, China

*Corresponding author: Areeba Rehman
Email: areebarehman453@gmail.com

Cite this Article:
Rehman, A., Ashraf, S., Tariq, S., Waleed, M., Khalid, H., Mazhar, H., Islam, N., & Munir, B. (2026). Geospatial assessment of land use/land cover change and land surface temperature dynamics using multi-index analysis and CA-Markov modeling from 1990-2022 in Lahore, Pakistan. *SciNex Journal of Advanced Sciences*, *1*(1), 42–65.

ABSTRACT:
The rapid urbanization has notably changed land use/ land cover (LULC) patterns of South Asian megacities, which intensifies the temperature of the land surface (LST) and urban heat islands. The consequences of urbanization on the climate and environment are critical for the natural resource management. This study examines long-term LULC dynamics and its effect on LST in Lahore, Pakistan, between 1990 and 2022 using multi-temporal Landsat data, various spectral indices and CA-Markov model to further predict future changes. Findings indicate that the vegetation cover decreased by about 71% in 1990 to 45.53% in 2022, with the settlement areas increasing by 13.54 to 36.78%. The overall accuracy of images ranged from 89 to 90%. Correspondingly, mean LST increased from 30 ºC up to more than 50 ºC. The correlation analysis showed that NDVI had strong negative correlation with LST but NDBI, NDBaI and NDWI and Urban Index had strong positive correlation with LST, demonstrating the importance of impervious and barren areas in intensifying heat. According to CA-Markov projections, settlement areas could increase more than 45% of the total area by 2050 with a further decrease in vegetation to almost 37%. These findings underline the importance of urban planning and sustainable land management that is climate sensitive so that the future thermal stress of rapidly growing cities can be reduced. The research also presents the understanding of LULC dynamics and promoting dialogs about the Sustainable Development Goals (SDGs)-climate action and building resilient cities and communities.

KEYWORDS:
LST; Urbanization; LULC; Urban heat island; CA Markov.

Received:29 December 2025 / Revised: 04 March 2026 / Accepted: 15 March 2026 / Published Online: 31 March 2026

INTRODUCTION

Globally, urban temperatures are progressively rising. Pakistan's urban population has increased significantly in recent years (Siddique et al., 2020). Land Use Land Cover (LULC) has changed as a result of urban development as building areas develop to meet the expanding population (Zhao & Miao, 2022). In the present moment, this change is essential. LULC is affected by all changes in climate change and endangered natural balances (Mumtaz et al., 2020). Urbanization is one of the key factors of LULC change, and it is critical to alter the Land Surface Temperature (LST) (Kaiser et al., 2022). The impacts of shifting agricultural borders, increasing urbanization and population expansion are not limited to a specific region (Liu et al., 2022).

The rapid urbanization causes the Urban Heat Islands (UHI) effect that disturbs the energy balance of the local environment (Singh et al., 2023). This effect is observed when the surface temperature of the metropolitan areas is greater than the surrounding areas. This change in LULC is one of the primary causes of UHI, as it increases the ability

Copyright (c) 2026 Author(s)
This work is licensed under a Creative Commons Attribution 4.0 International License.

to store heat and forms more impermeable surfaces (Tan et al., 2020). Some of the adverse effects of UHI intensification include unpredictable rainfall, health issues, natural disasters such as floods, and poor air quality (Traore et al., 2021). Also, LULC changes may influence the urban microclimate and LST variation (Demisse Negesse et al., 2024).

LULC is highly affected by radiation and LST in the local and regional contexts. It has been repeatedly demonstrated that variations in LULC, particularly in urban centers, relate to rises in LST (Karakuş, 2019; Negesse et al., 2024). In many studies, it has been found that high LST and area radiation can have severe adverse health impact (Dutta et al., 2019; Ramzan et al., 2022; Ullah et al., 2023). These health effects manifest themselves in a number of ways but a few of them include the thermal comfort index, discomfort index, and temperature relative index (Tarasov & Rakhmanov, 2023). A global average of LST rose by 0.6 to 0.9 ºC between 1960 and 2015 (Hussain et al., 2023; Qureshi et al., 2023). Thus, fluctuations in LST that are consistent with global radiation should be continuously observed, especially in urban environments (Shiflett et al., 2017). This monitoring helps in planning efficient adaptation and mitigation strategies.

Urban expansion has affected the growth of rural areas and societies, the transformation of the climate and LULC (Rees et al., 2024). The LULC changes need to be analyzed to address environmental issues such as heat islands, flooding, loss of biodiversity, loss of arable land, local warming, decline of the ecosystem, and loss of habitat (Mir et al., 2025). The overall health of our environment is highly jeopardized unless the changes in LULC and their impacts on LST are resolved. The analysis of the relationship between LST and LULC aims to address specific problems in the ecosystems of the region and deepen our understanding of the impact of LST on the environment (Feng et al., 2025). The photosynthetic activity, based on the Normalized Difference Vegetation Index (NDVI) is related to the biological mass of plants, water stress and biodiversity (Ekaputri et al., 2024).

The NDVI has been increasingly preferred as a method of elucidating the spatiotemporal aspects of LULC in the past few years. NDVI values have been widely used in remote sensing (RS) research to identify and analyze vegetation patterns (Dutta et al., 2022). The Normalized Difference Built-up Index (NDBI) has been essential for determining the concentration and growth of urban areas, whereas the NDVI tool has been helpful in determining vegetation areas (Yasin et al., 2022). Research on the Normalized Difference Barren Index (NDBaI), Normalized Difference Water Index (NDWI) and Urban Index (UI) indicates that there is very little correlation between the NDVI and LST area. NDVI decreases when vegetation areas disappear, but NDBI rises as built-up areas grow (Zheng et al., 2021). These factors have a significant impact on LST fluctuations due to LULC changes. For urban modeling, LULC mapping, and evaluating the environmental effects of urban growth over particular time periods, integrating GIS and RS is a useful method (Azizi et al., 2022). RS and GIS-derived spatial data is a cost-effective method that offers precise and fast information regarding degraded areas during specific times (Meer & Mishra, 2020). Recent LULC studies have pointed out the importance of focusing on specific locations (Rafiq et al., 2018; Shahid & Venturi, 2025). In LULC research, some locations are frequently ignored. The topography of the study area and its varied ecosystems render the area a vital study site where the local effects of LULC changes can be studied.

Even though research on LULC change and LST dynamics in Pakistan has been increasing, much of this work is conducted at shorter time scales, at a single spectral index, or in other cities than Lahore, with little combination of future land-use simulations. The existing research on Lahore focusses on LULC or LST a lot, without a combination of the multi-index analysis and long-term projection models. To fill this gap, the current study will combine over thirty years of Landsat data with multiple spectral indices and CA-Markov modeling to study previous trends and predict future interactions between LULC and LST. This combined method will give a deeper insight into the thermal processes of the city of Lahore than earlier national-scale research.

The major aims of the research are (i) to examine the LULC changes from 1990 to 2022 in Lahore. (ii) to identify the correlation among NDVI, NDBI, NDBaI, NDWI, and UI with LST. (iii) to determine the future LULC patterns by 2050 using CA-Markov modeling to assess the potential implications on urban thermal environments.

The findings aim to identify the reasons that are contributing to Lahore's declining green space over time, emphasize those factors in future prediction maps, and make recommendations for implementing sensible land-use policies.

METHODOLOGY

Study Area

With a population of 11.13 million as per census of 2017, Lahore ranks as the 26th most populous city in the world and the second largest metropolis in Pakistan after Karachi (Ali et al., 2022). It is the largest city in the province of Punjab, which it serves as the capital of. The district is bordered to the northeast by India, to the west by Nankana Sahib, to the

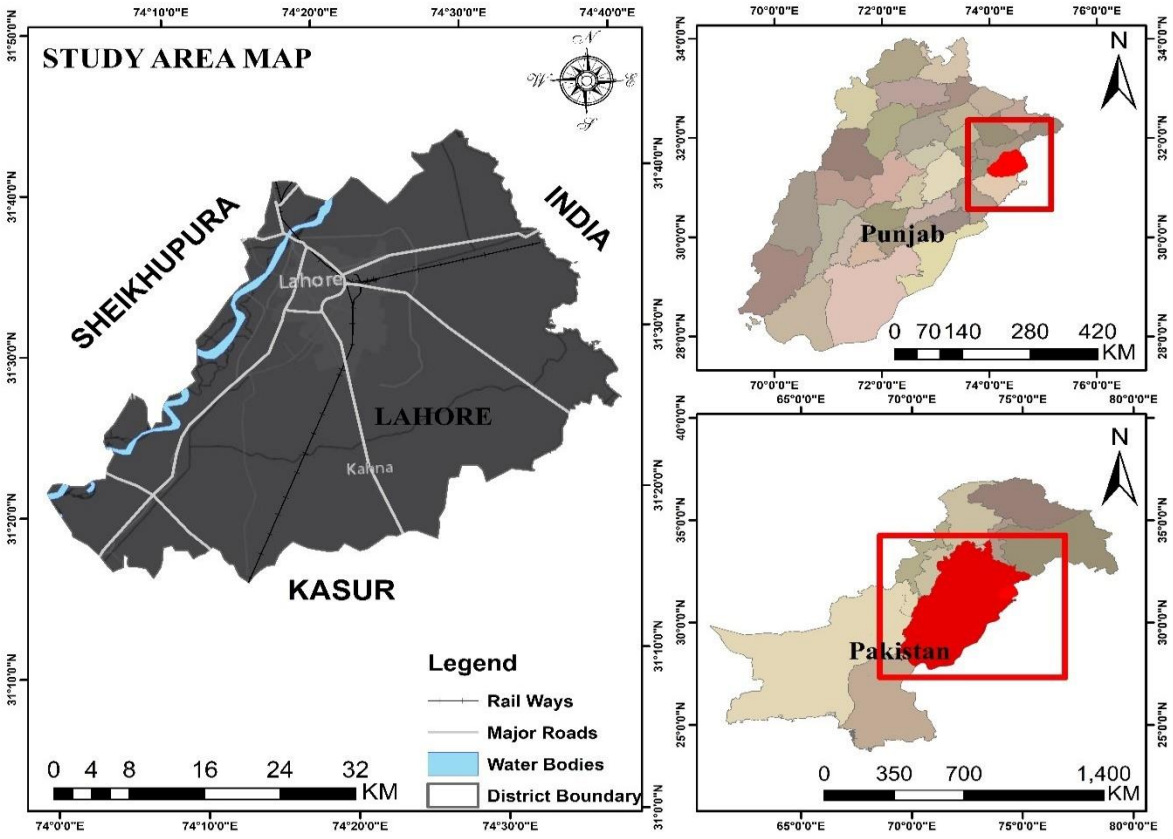

Figure 1: Location of study area (Lahore city) in the map of Punjab Province, Pakistan.

northwest by Sheikhupura District, and to the south by Kasur District. The district of Lahore is located between latitudes 31°42' 18 N and 31°15' 33 N, and longitudes 74°39' 31 E and 74° 1' 23 E, in terms of geography. It has semi-arid to subtropical climate, hot in summer and mild in winter. The average yearly temperature is 24-26 ºC, and summer temperatures tend to reach 45 ºC, and average annual rainfall is around 600-700 mm. The study area was selected on the basis of fast urban growth, dense population, susceptible to urban heat stress and facing unplanned urbanization.

Data Collection

The effects of LULC variations on Lahore city's LST were examined through the processing of satellite imagery. Table 1 provides specifics about the satellite data that was downloaded and prepared for study. For the years of 1990, 1995, 2000, 2005, 2010, 2015 and 2022, satellite imagery was obtained from the website https://earthexplorer.usgs.gov/ to examine how LULC affected seasonal temperature fluctuation. The availability of satellite data and cloud cover are related to the variation in the picture acquisition date (Tariq & Shu, 2020). The pre-monsoon period (May) was selected as the satellite acquisition period to reduce cloud cover and seasonal change in vegetation and surface temperature. The images that had a cloud cover of less than 10% were given priority to make the comparison across years to be consistent and reliable.

Table 1: Summary of the Landsat data collected for processing (at < 10% cloud cover).

Year	Sensor	Path/Row	Date	Bands for LULC
1990	Landsat 5 TM	149/37	12 May 1990	2 (Green), 3 (Red), 4 (NIR)
1995	Landsat 5 TM	149/37	18 May 1995	2 (Green), 3 (Red), 4 (NIR)
2000	Landsat 5 TM	149/37	14 May 2000	2 (Green), 3 (Red), 4 (NIR)
2005	Landsat 7 ETM+	149/37	20 May 2005	2 (Green), 3 (Red), 4 (NIR)
2010	Landsat 7 ETM+	149/37	16 May 2010	2 (Green), 3 (Red), 4 (NIR)
2015	Landsat 8 OLI/TIRS	149/37	09 May 2015	3 (Green), 4 (Red), 5 (NIR)

Copyright (c) 2026 Author(s)
This work is licensed under a Creative Commons Attribution 4.0 International License.

2022	Landsat 8 OLI/TIRS	149/37	07 May 2022	3 (Green), 4 (Red), 5 (NIR)

Meteorological and environmental variables were taken into account when downloading satellite data for a particular date to rule out the effects of rainy weather, climatic, anthropogenic, and biochemical influences on image quality. Satellite data collected at various places and times were normalized using atmospheric, radiometric, and sun elevation corrections. The Landsat toolbox was used to eliminate the scan line errors in the Landsat 7 data. In order to accomplish this, raster data including scan lines was imported, the Fix Landsat 7 Scanline Error tool was used, and the scan lines were eliminated prior to any processing. LULC maps were then created by processing the satellite data. LST was retrieved from thermal bands using ArcMap (v. 10.7). In the IDRISI SELVA, LULC prediction for 2050 were also made.

Data Processing

Image Analysis

LULC classification is essential for detecting changes in land use and cover during the study's specified time frame. LULC changes are mapped using Landsat imagery for the years 1990–2022. The images were grouped into four categories: vegetation, settlement, barren land, and water feature The Maximum Likelihood Classification algorithm was used to perform supervised classification. Visual interpretation of Landsat imagery, high resolution Google Earth imagery and field knowledge were used to select training samples that represented spectral signatures of each class. A total of about 250 training samples per image were used, which encompassed vegetation, settlement, barren land and water bodies. The accuracy of classification was determined using stratified random sampling of 40 validation points per class, the overall and Kappa coefficients were computed to determine the classification performance (Haque & Basak, 2017).

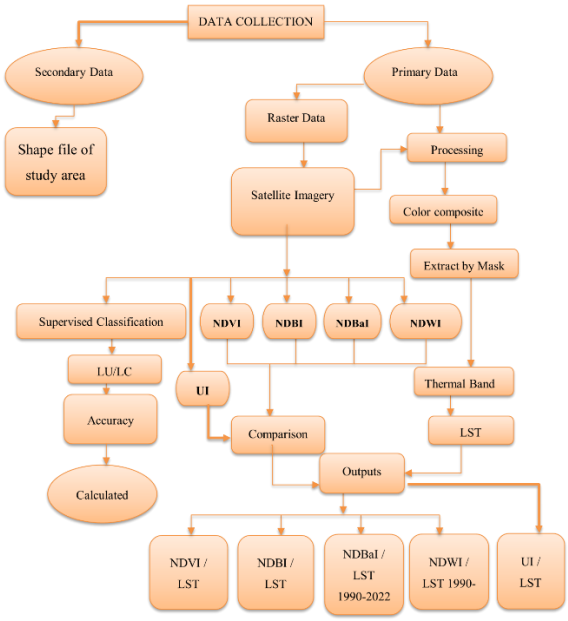

Figure 2: Methodological framework used in this study.

Markov Chain

A Markov chain model is a stochastic model that shows a sequence of possible events in which the probability of each event depends only on the state reached by the one before it. The classified images of 1990 and 2022 are then used by the Markov chain extension of LCM (IDRISI Selva), which creates a transition probability image of a certain time by using an earlier and later date picture. For the development of our study's transition probability map for 2050 (Abdulrahman & Ameen, 2020). The CA-Markov model is based on the assumption that future transitions of land-use will be based on the historical probabilities of change and spatial neighborhood impacts but that socio-economic drivers are implicitly remain constant. Though this method does not directly consider changes in policy or the demographics, it gives a probabilistic model upon which future LULC patterns can be projected under the current trends.

Extraction of LST from Thermal Bands

The land surface temperature must be ascertained by converting the sensor data into a physical quantity because a sensor captures the electromagnetic radiation intensity for every pixel as a numerical value. Through the conversion of the DNs into more practical actual quantities, such as brightness temperature, reflectance or radiance. The land surface temperature was calculated using the method below using the Landsat images' thermal bands. Thermal electromagnetic energy is released by any item that has a temperature higher than absolute zero (k). Using the irradiance scaling factors listed in the metadata file, thermal sensor data was transformed to sensor-level radiance (Wu et

al., 2010). Following this banding, the thermal constants given in the metadata are used to transform the data from spectral luminance to upper atmospheric luminance temperature.

The spectral radiance was calculated by the following equation 1.

$$L_\lambda = M_L Q_{cal} + A_L \quad 1$$

Where Q is the quantized and calibrated standard product pixel values (DN), L is the TOA spectral radiance (Watts/(m^2*srad*m)), ML is the band-specific multiplicative rescaling factor from the metadata (RADIANCE MULT BAND x), and AL is the band-specific additive rescaling factor from the metadata (RADIANCE ADD BAND x). Formula then uses the thermal constants given in the metadata file to transform band data from spectral radiance to top of atmospheric brightness temperature.
The brightness temperature was calculated by equation 2.

$$Tb = K2 / \ln(k1/l\lambda + 1) \quad 2$$

As stated by Jimenez-Munoz et al. (2014), T or BT stands for top of atmosphere brightness temperature (K); Lλ is TOA spectral radiance (Watts/(m2 * srad * μm); K1 is the band-specific thermal conversion constant from the metadata (K1_CONSTANT_BAND_x, where x is the thermal band number); and K2 is the band-specific thermal conversion constant from the metadata (K2_CONSTANT_BAND_x, where x is the thermal band number). A single thermal band from a data collection is used in a single channel technique to get the earth's surface temperature. Consequently, adjustments are required for the earth's surface emissivity since the temperatures determined using the aforementioned method pertain to a black body. The normalized differentiated vegetative index is used to calculate the emissivity by applying an equation 3.

$$LST = Tb/[1 + \{(\lambda * Tb/\rho) * \ln\epsilon\}] \quad 3$$

p is the Planck's constant (6.626 * 1034 J s), s is the Boltzmann constant, c is the speed of light (2.998 108 m/s), e is the emissivity, Tb is the at-satellite temperature, and w is the emission wavelength (Teimouri & Karbasi, 2024).

All the variables and symbols in the LST retrieval equations were standardized in the Landsat metadata documentation and NDVI based emissivity correction was used to convert brightness temperature to land surface temperature.

The ratio of the energy emitted by a material surface to that emitted by a black substance, or ideal emitter, under identical temperature, wavelength, and dark conditions is known as LSE, or Earth's surface emissivity. The equation 4 was used to calculate it:

$$LSE = 0.004 * Pv + 0.986 \quad 4$$

The PV (percentage of vegetation), which is closely linked to the emissivity (ε), has to be determined using the NDVI. Equation 5 and 6 was used to calculate the PV.

$$P_v = \left(\frac{NDVI - NDVI_{min}}{NDVI_{max} - NDVI_{min}}\right)^2 \quad 5$$

Lastly, using the formula 0 degrees Celsius equals 273.15K, the retrieved LST's Kelvin unit can be converted to Celsius. The following equation 6 was used to do this.

$$LST - 273.15 \quad 6$$

Computation of NDVI, NDBI, NDBaI, NDWI and UI

Normalized Difference Vegetation Index (NDVI)

The Normalized Differential Vegetation Index or NDVI, is a crucial indication of the built environment that is used in remote sensing to assess whether or not green vegetation is present in the objective reality that is being collected. To stabilize irregular radiation patterns like mountains and haze shading, it normalizes the NIR-RED/NIR+RED alteration. For this investigation, NIR and Red Band Landsat images are utilized (Robinson et al., 2017). The NDVI was determined by equation 7.

$$NDVI=(NIR-RED)/(NIR+RED) \quad 7$$

Normalized Difference Built Up Index (NDBI)

Normalized differentiated built-up index, extract, and identify built-up or urban regions from imagery (Sinha et al., 2016). It utilizes the near- and mid-infrared wavelengths of reflection. The NDBI was determined by equation 8.

$$NDBI=(MIR-NIR)/(MIR+NIR) \quad 8$$

Normalized Difference Barren Index (NDBaI)

The environment depends heavily on bare plains. Hung utilized it to analyze the spectral properties of various LULC. It can also be applied to the classification of bare terrain. Lands that are left bare quickly gain and lose heat. It makes use of thermal infrared and shortwave reflectivity (Hung, 2020). The NDBaI was determined by equation 9.

Copyright (c) 2026 Author(s)
This work is licensed under a Creative Commons Attribution 4.0 International License.

NDBaI=(SWIR-TIRS)/(SWIR+TIRS) 9

Normalized Difference Water Index (NDWI)

Normalize the water's differential index and investigate water bodies using NIR and SWIR. NDWI enhances water expertise in numerous instances. The water scene feature was enhanced using NDWI (Singh et al., 2015). The NDWI was determined by equation 10.

NDWI=(NIR-SWIR)/(NIR+SWIR) 10

Urban Index (UI)

Urban Index transformation generates a density map using VNIR and SWIR. The density of settlements can be described by remote sensing using spectral transformation (Zhang et al., 2017). It was made with the following equation 11.

UI=(SWIR-VNIR)/(SWIR+VNIR+1) 11

Table 2: Land Use-Land Cover Classes area (Km^2) of Lahore (1990-2022).

Year	Vegetation Area/%	Settlement Area/%	Barren Land Area/%	Water Body Area/%
1990	1211.4972 / 71.978	227.9601 / 13.543	235.5372 / 13.993	8.1396 / 0.4835
1995	1211.497 / 71.978	247.9601 / 14.732	215.5372 / 12.805	8.1396 / 0.4835
2000	1106.056 / 65.714	265.974 / 15.802	295.248 / 17.541	15.585 / 0.942
2005	1129.487 / 67.106	356.7357 / 21.194	189.378 / 11.251	7.5339 / 0.447
2010	1059.339 / 62.938	407.111 / 24.187	204.795 / 12.1675	11.887 / 0.7062
2015	789.965 / 46.934	420.521 / 24.984	460.359 / 27.351	12.2886 / 0.7301
2022	766.3239 / 45.529	618.975 / 36.775	284.643 / 16.911	13.191 / 0.783

RESULTS

Land Use Land Change (LULC) Variation (1990-2022)

Activities in vegetation, populated areas, and arid regions have changed as a result of urbanization and other human activities. According to Table 2, the estimated areas of vegetation in 1990, 1995, 2000, 2005, 2010, 2015, and 2020 were 1211, 1106, 1129, 1059, 789, and 766 km^2, respectively. Vegetation has decreased from 71% to 45% of the overall area over the last three decades. Because of harvesting and re-cultivation in the study region as a result of the area being converted for residential and commercial use, the amount of vegetation area has significantly decreased in the middle of the year. Since the start of the study period, the settlement area, which was 227 km^2 in 1990, has grown to 247 km^2 in 1995, 265 km^2 in 2000, 356 km^2 in 2005, 407 km^2 in 2010, and 420 to 618 km^2 constructed in 2015–2022. Development has grown from 0.97% to 8% of Lahore's overall territory in recent decades (Figure 3). Urbanization, or the unplanned division of land use patterns, and industrial growth are the causes of this notable increase. The barren zone shows a slight variation with 13%, 12%, 11%, 17%, 12%, 27% and 16%.

To assess the accuracy of the graded images, 40 random samples have been taken from each class and a total of 160 samples from each image. Overall accuracies ranged from 0.91 for 1995-2000, 0.925 for 2005, 0.90, 0.91 and 0.90 for 2010, 2015, 2022 (Hugenholtz et al., 2013). With kappa coefficients of 0.89, 0.89, 0.89, 0.90, 0.87, 0.89 and 0.87. Table 3, shows kappa coefficients of 0.89, 0.89, 0.89, 0.90, 0.87, 0.89, and 0.87. The kappa coefficient is a method for calculating a classifier's percentage improvement on a totally random set of classes. The accuracy of the result belongs to the threshold value the was assigned by many of the researcher as if the image accuracy in Kappa and Overall is higher than 0.6 then it will be considered as correct classification (Ahmed et al., 2013). The values of the results are higher than 0.6, which shows the reliability of the results.

Accuracy Assessment of LULC Variation

Table 3: Accuracy Assessment of classified image 1990-2022.

Image Years	Overall Accuracy in Percentage	Kappa coefficient
1990	0.91875	0.894137258
1995	0.91546	0.894228324
2000	0.912374	0.893462516
2005	0.925	0.902245303
2010	0.90625	0.878524067
2015	0.91357	0.894337233
2022	0.90423	0.877413056

Markov Chain Analysis

To comprehend the likely change in LULC up to 2050, a transition probability picture has been constructed using the Markov chain model, as shown in Figure 4. Vegetation degradation and increasing in settlements provide the most potential for change in Land use- Land cover. Due to urbanization and global warming arid zones that have

converted from vegetation to build up are more likely to migrate to the Land Use-Land cover model (Hamad et al., 2018).

Table 4: Transition probability values of the predicted area in 2050.

Classes	Predicted area in (2050)	Percentage of total area
Vegetation	631.2429	37.50401706
Settlement	766.701	45.55198543
Barren Land	267.0489	15.86616895
Water Body	18.1413	1.077828558

Copyright (c) 2026 Author(s)
This work is licensed under a Creative Commons Attribution 4.0 International License.

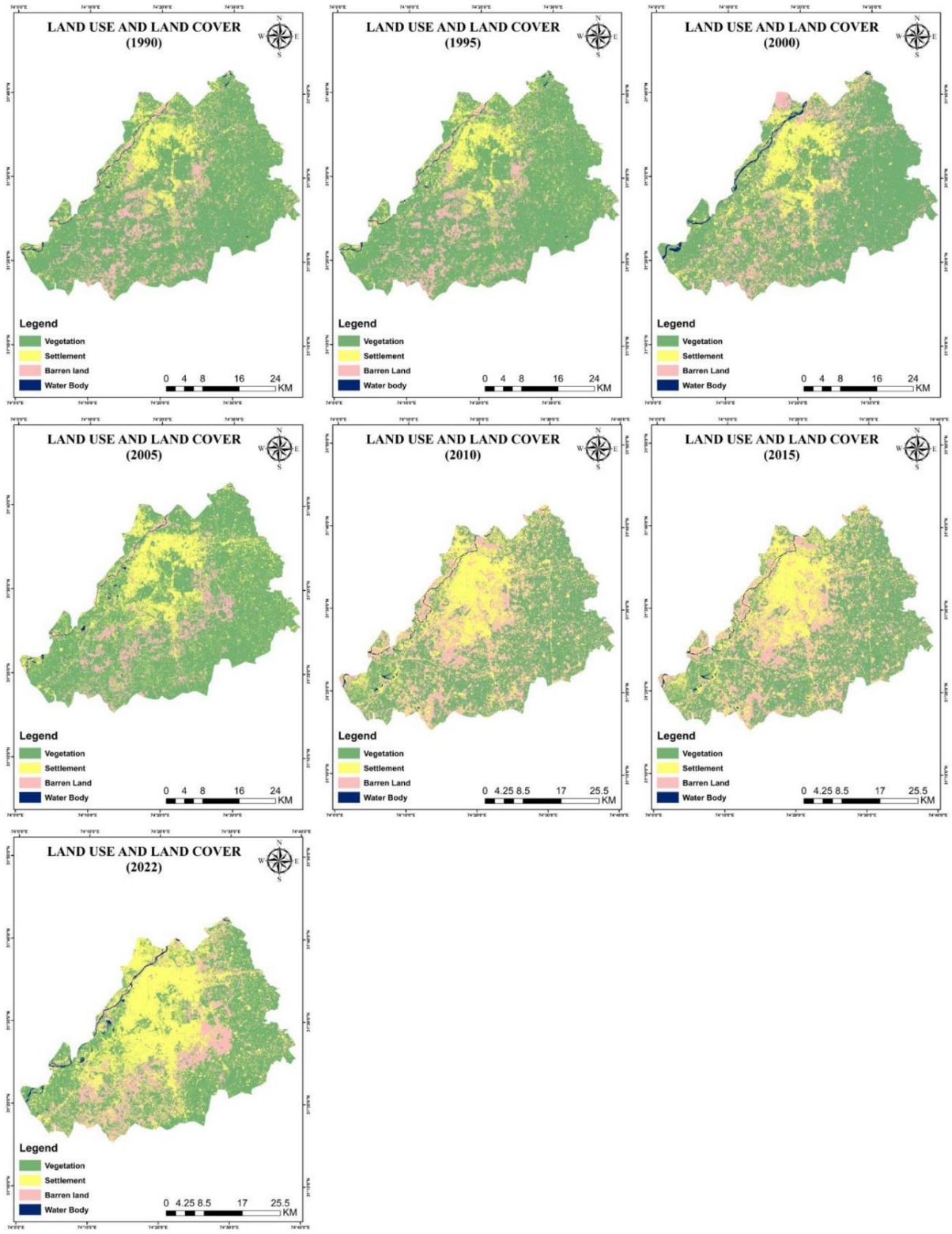

Figure 3: Land Use-Land Cover Classes from 1990 to 2022 of study area.

Land Surface Temperature (LST)

The LST was approximately 30.0 C in 1990, 33.0 C in 1995, 37.0 C in 2000, and 39.0 C in 2005. Furthermore, it was found that the land area's temperatures in 2010, 2015, and 2022 were 48, 49, and 51 degrees. April 2018 was the 400th consecutive month with an above-average temperature, meaning 1984 was the last year, according to a recent report by NOAA's National Environmental Information Centers, which claims that the Earth shattered the climate record by entering the worst-case scenario. The earth's temperature was below average, and it is on track to reach the degrees Celsius of climate change (NCEI, 2017).

The district's average temperature variance since 1990 has been 3 degrees Celsius, which further supports our findings. As seen in Figure 5, the LST, which was derived from the most recent satellite data, indicated that the dry and urban regions were the source of the highest temperature. In order to determine which features, generate the most heat, places with the greatest temperatures have been identified using last

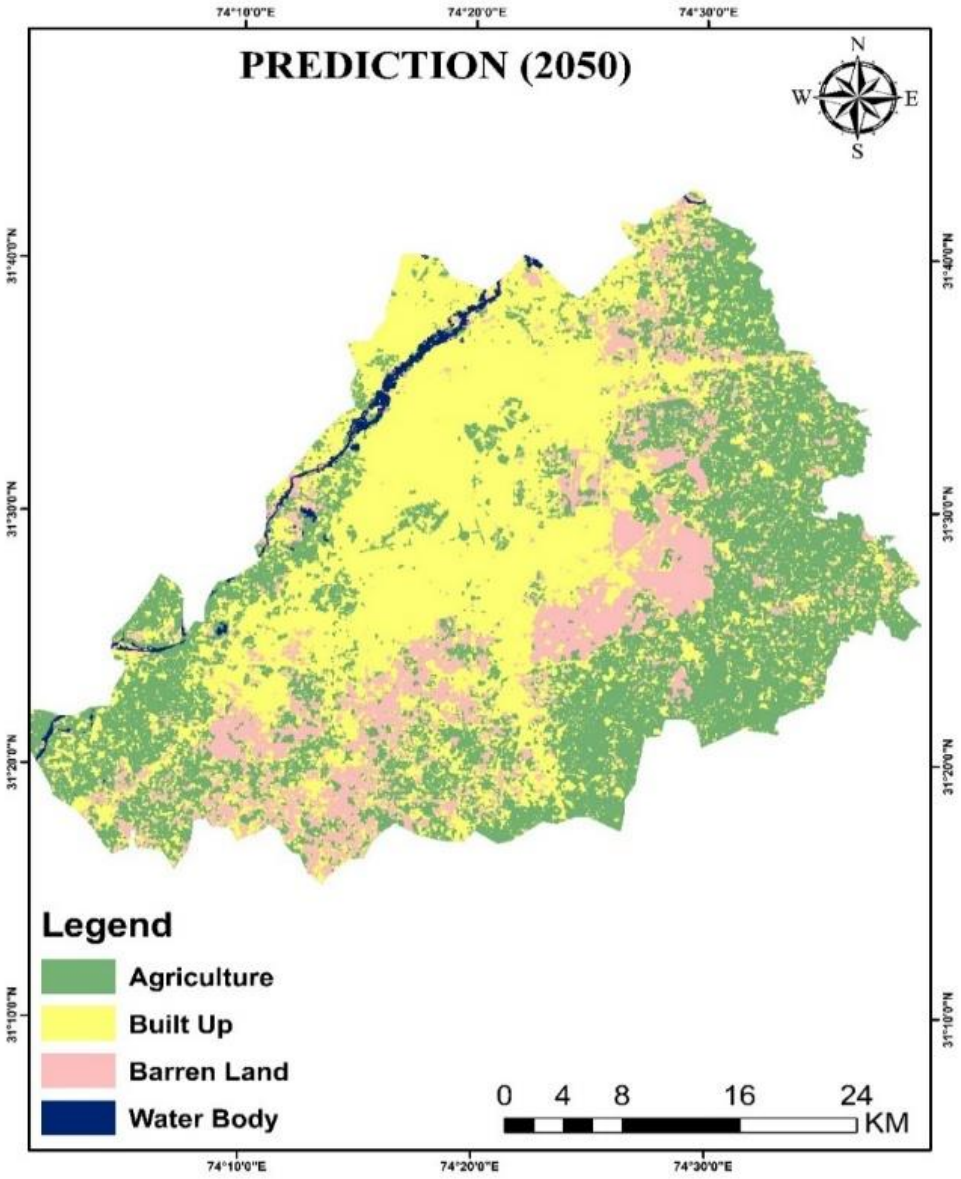

Figure 4: Transition Probability Map of Lahore (2050).

Copyright (c) 2026 Author(s)
This work is licensed under a Creative Commons Attribution 4.0 International License.

year's LST. Samples of those areas will then be collected and superimposed with Google Earth images.

Normalized Difference Vegetation Index (NDVI)

The NDVI has been used to determine the vegetation's health based on the difference between the red and near-infrared bands. The red and near-infrared bands are used to compute the NDVI. The range of the NDVI value was between -0.28 and 0.66 in 1990 and between -0.3 and 0.62 in 1995. The

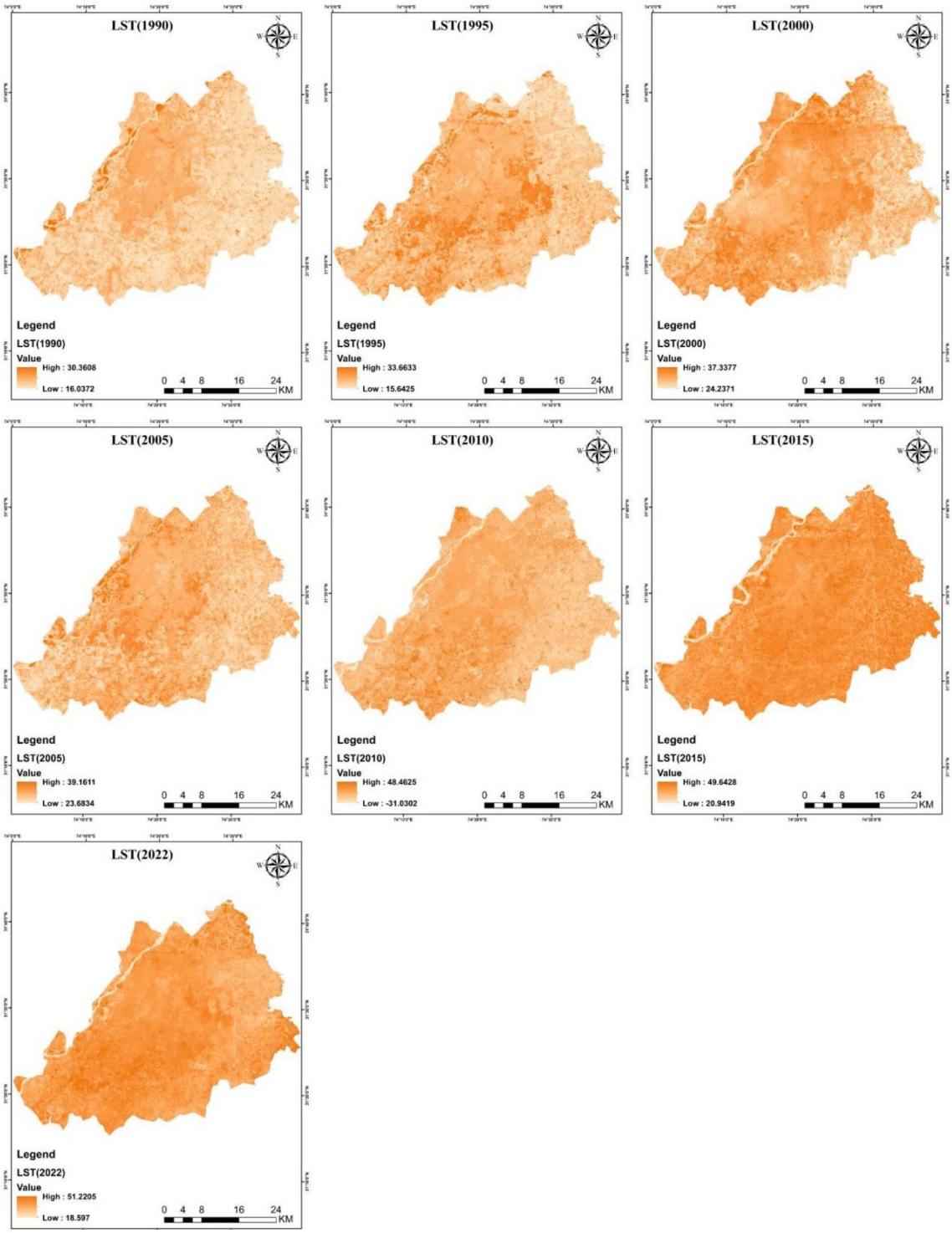

Figure 5: Spatial distribution of LST over Lahore from 1990 to 2022.

NDVI ranged from -0.3 to 0.6 in 2000, from -0.15 to 0.58 between 2005 and 2010 and from -0.32 to 0.57 in 2015 and 2022 (Figure 6). The NDVI has decreased during the past three decades as a result of land conversion to built-up areas. Although a comparison with LST shows that LST increases as vegetation cover diminishes, the NDVI has clearly changed. The density of the vegetation has affected the LST intensity. Less intense plant cover is not as effective in

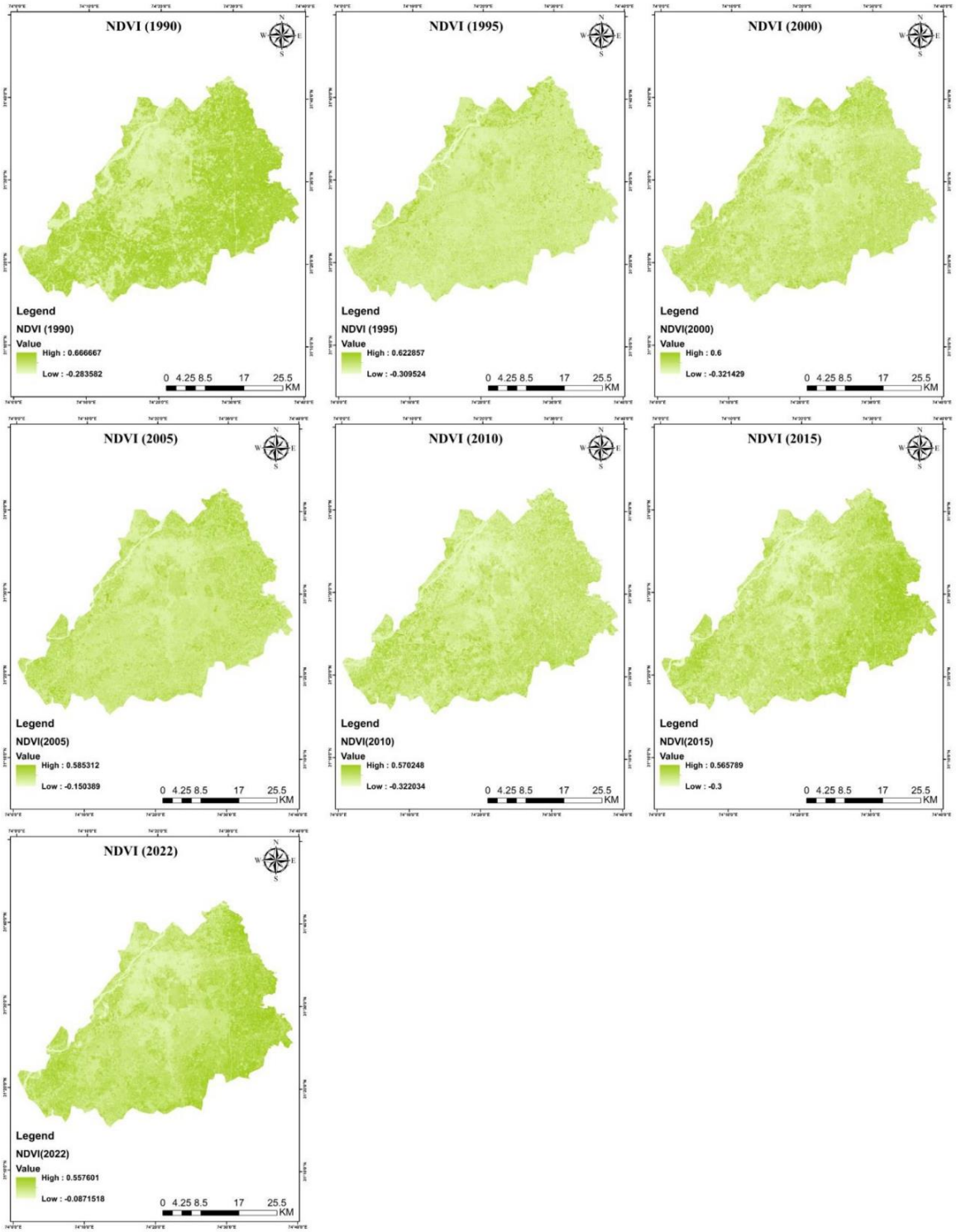

Figure 6: Spatial distribution of NDVI over Lahore from 1990 to 2022.

Copyright (c) 2026 Author(s)
This work is licensed under a Creative Commons Attribution 4.0 International License.

Figure 7: The correlation plots between NDVI and LST (1990-2022) in the Lahore city.

controlling the development of intense soil surface temperature as rich plant cover. The maps illustrate the evolution of vegetation density over time, as seen in Figure 6. Because of urbanization, lower NDVI values indicate less vegetation cover, whereas high NDVI values show dense plant cover. As vegetation density decreases, temperatures

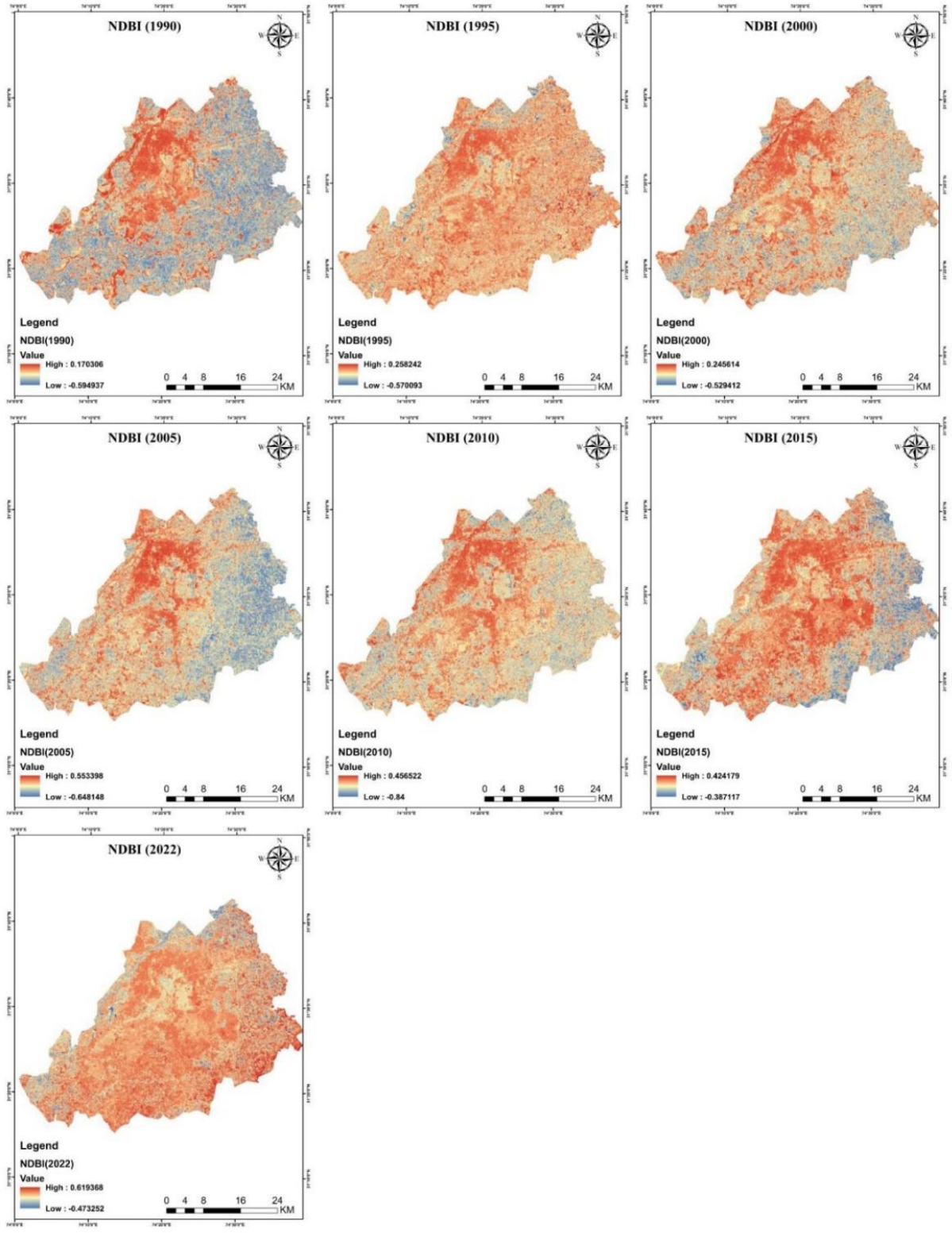

Figure 8: Spatial distribution of NDBI over Lahore from 1990-2022.

rise. Additionally, the relationship was 0.88 in 1990, 0.88 in 1995, 0.82 in 2000, and 0.76, 0.74, 0.92, and 0.71 from 2005 to 2022; respectively (Figure 7). In all situations, the association is substantial; however, because vegetation is

Copyright (c) 2026 Author(s)
This work is licensed under a Creative Commons Attribution 4.0 International License.

significantly associated with lower LST levels, the relationship is reversed. Correlation analysis always reports correlation coefficients (r) to have consistent statistical interpretation across indices and years of study.

Normalized Difference Built Up Index (NDBI)

The normalized difference built up index is used to intensify settlement data and extract the built area from urban land use. A densely populated area is indicated by high NDBI readings. The NDBI varied from -0.59 to 0.17 in 1990, from -0.57 to 0.25 and -0.52 to 0.25 in 1995 and 2000, from -064 to 0.55 and -0.84 to 0.45 in 2005 and 2010, and from -0.38 to 0.45 and 0.47 to 0.61 between 2015 and 2022. The NDBI value was occasionally rising in some places where the vegetation was disturbed by rapidly expanding settlement. The maps in Figure 8 show the built-up area. The land surface temperature rises as the built-up area grows, according to a comparison between LST and NDBI. This is due to the fact that impermeable areas make up the majority of the inhabited centers. This is because impermeable zones make up the majority of the populous regions. Heat is produced in large quantities in urban areas because they use more energy than rural areas. High temperatures are caused by trapped heat and excessive energy use as the built-up area expands. The positive correlation between the NDBI and LST suggests that as the built-up area has increased, so has the earth's surface temperature. The relationship was 0.90 in 1990, 0.91 in 1995, 0.99 for 2000 and ranges from 0.81-0.97 for 2005, 2010, 2015 and 2022. The strong the relation

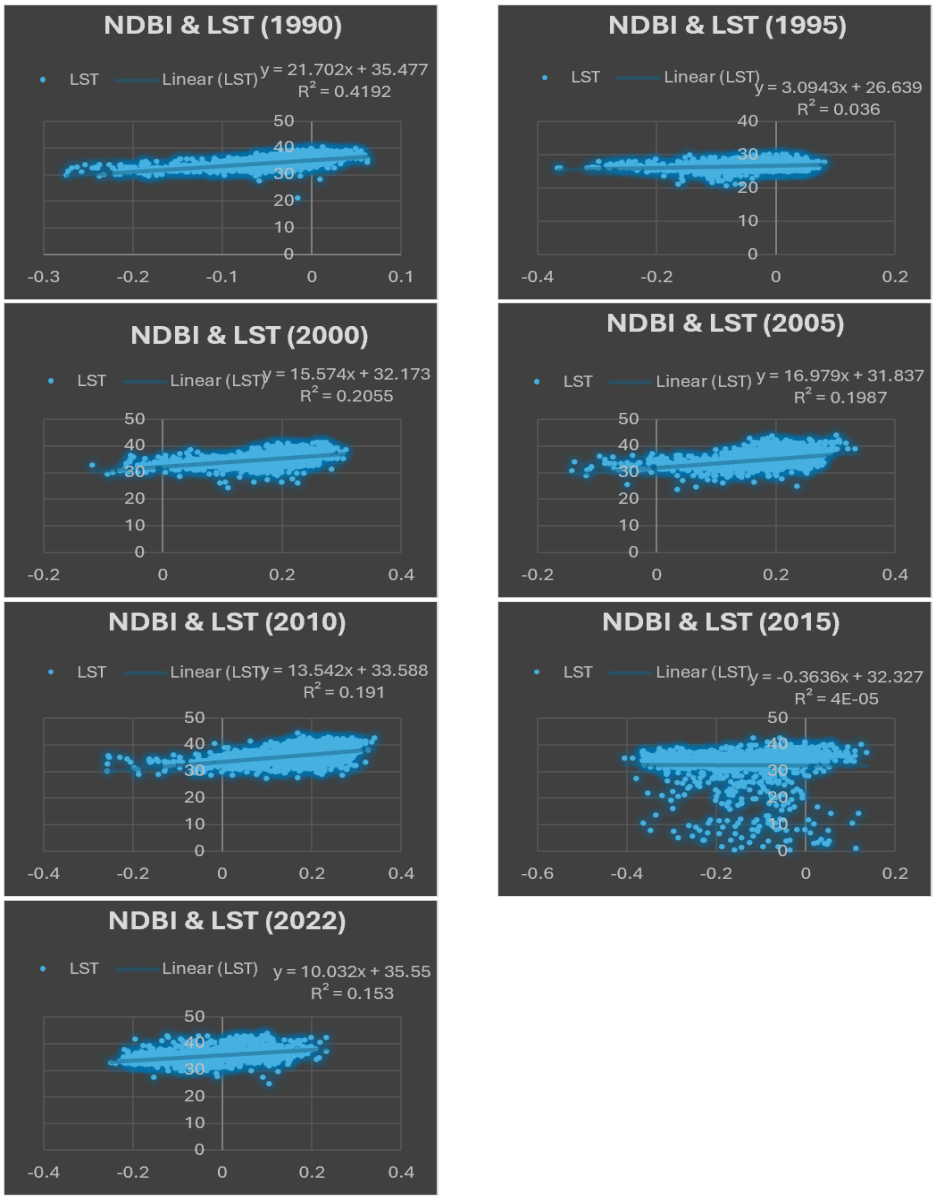

Figure 9: The correlation between NDBI and LST (1990-2022) in the Lahore city.

between the NDBI and LST, ss the NDBI is increased the LST of the area were also increased. Compared to rural settings, urban surroundings are more energy-intensive and have an impervious surface. Because of the large amount of stored heat and the high energy demand, the increased built-up area may result in high temperatures.

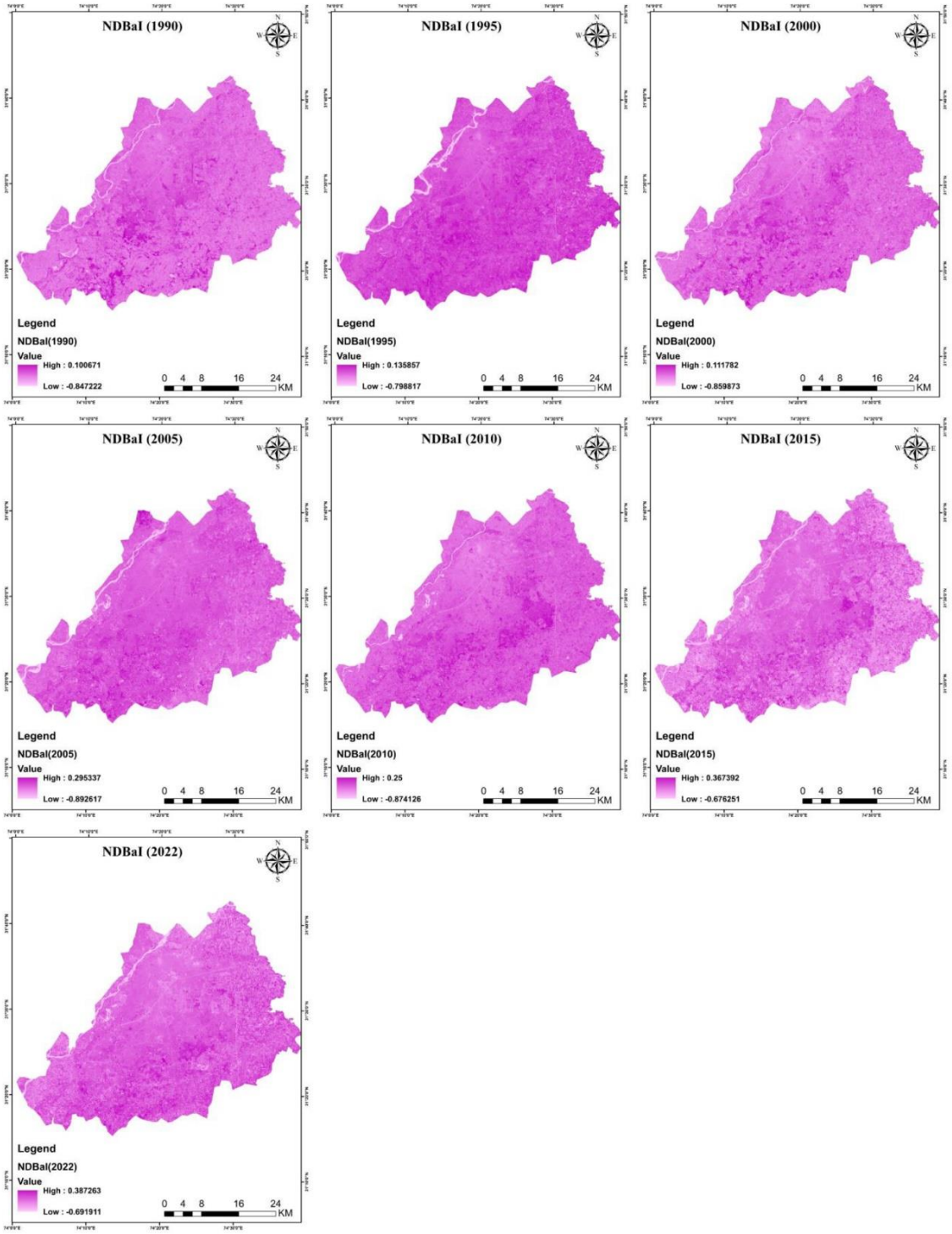

Figure 10: Spatial distribution of NDBaI over Lahore from 1990 to 2022.

Copyright (c) 2026 Author(s)
This work is licensed under a Creative Commons Attribution 4.0 International License.

Normalized Difference Barren Index (NDBaI)

NDBaI levels varied from -0.84 to 0.10 in 1990, from -0.79 to 0.13 in 1995, from -0.85 to 0.11 in 2000, from -0.89 to 0.29 and -0.87 to 0.25 in 2005 and 2010; in 2015 and 2022, NDBaI values varied from -0.67 to 0.36 to -069 to 0.38. This indicates that, as Figure 10 illustrates, desolate areas have changed since 1990. It is evident from comparing LST to NDBaI that the LST increases with the size of the barren zone. The larger surface area and infinite number of soil particles cause arid areas to retain water and radiate heat quickly. NDBaI and LST have a high positive correlation, which explains why LST increases with sterile zone size.

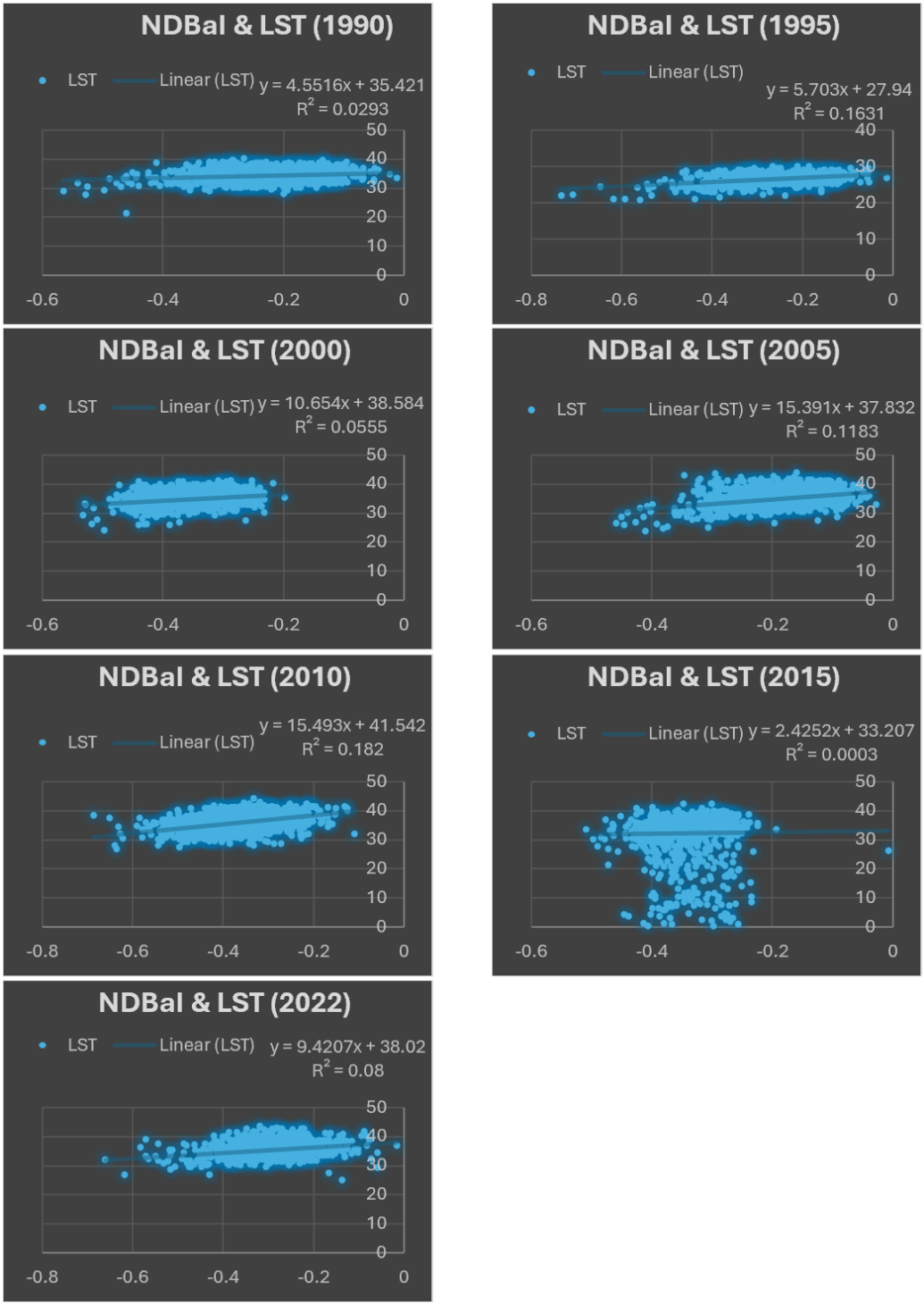

Figure 11: The correlation between NDBaI and LST (1990-2022) in the Lahore city.

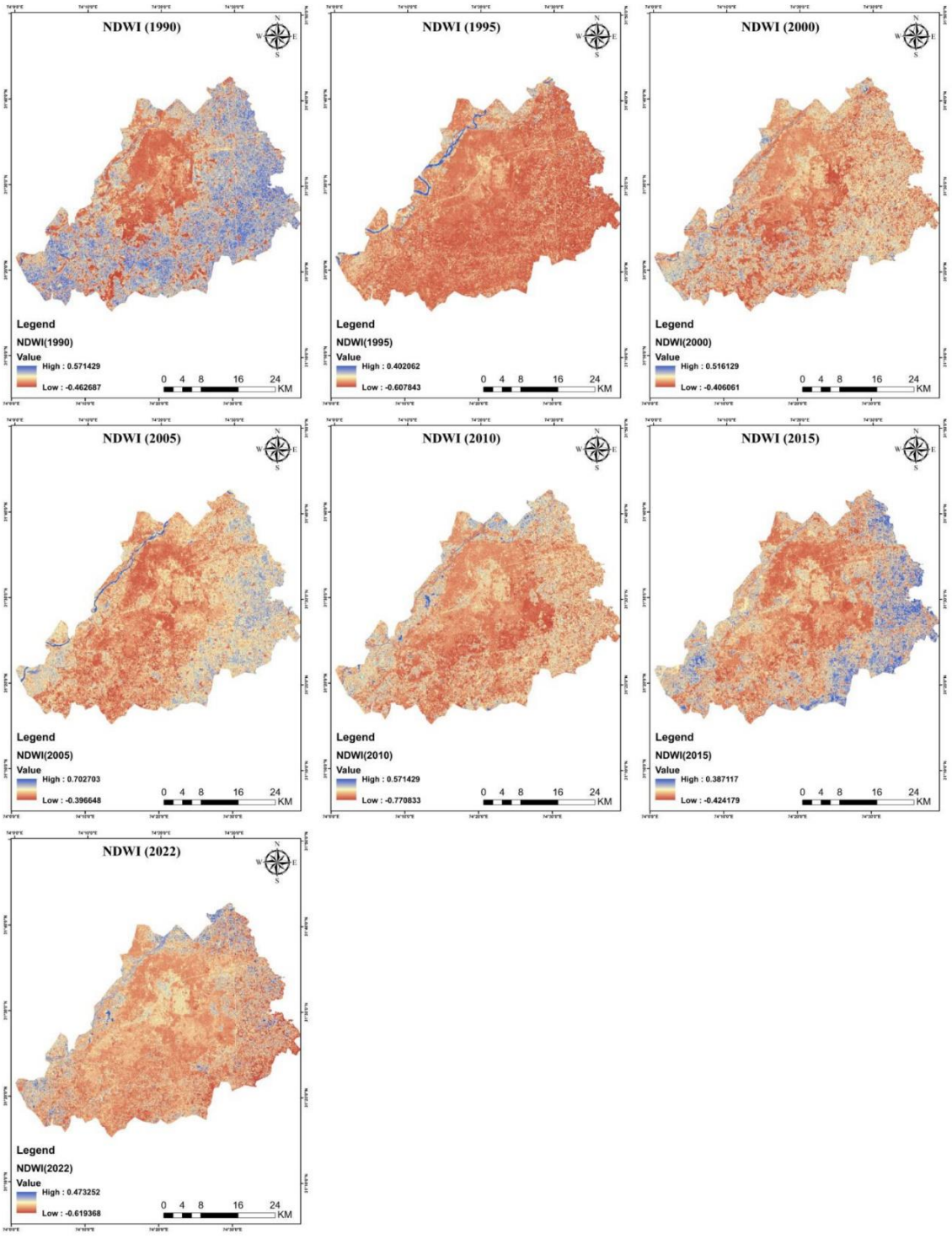

Figure 12: Spatial distribution of NDWI over Lahore from 1990 to 2022.

The correlation was 0.96, 0.96, 0.93, 0.97 in 1990, 1995, 2000, and 2005; it was 0.94 and 0.79 in 2010, 2015, and 0.96 in 2022 (Figure 11), with a larger sterile area. This is because sand particles do not compact in arid areas, and a large surface has the ability to release heat quickly; however, in arid areas that have solidified and contain moisture, soils tend to store heat longer due to the accumulation of heat.

Copyright (c) 2026 Author(s)
This work is licensed under a Creative Commons Attribution 4.0 International License.

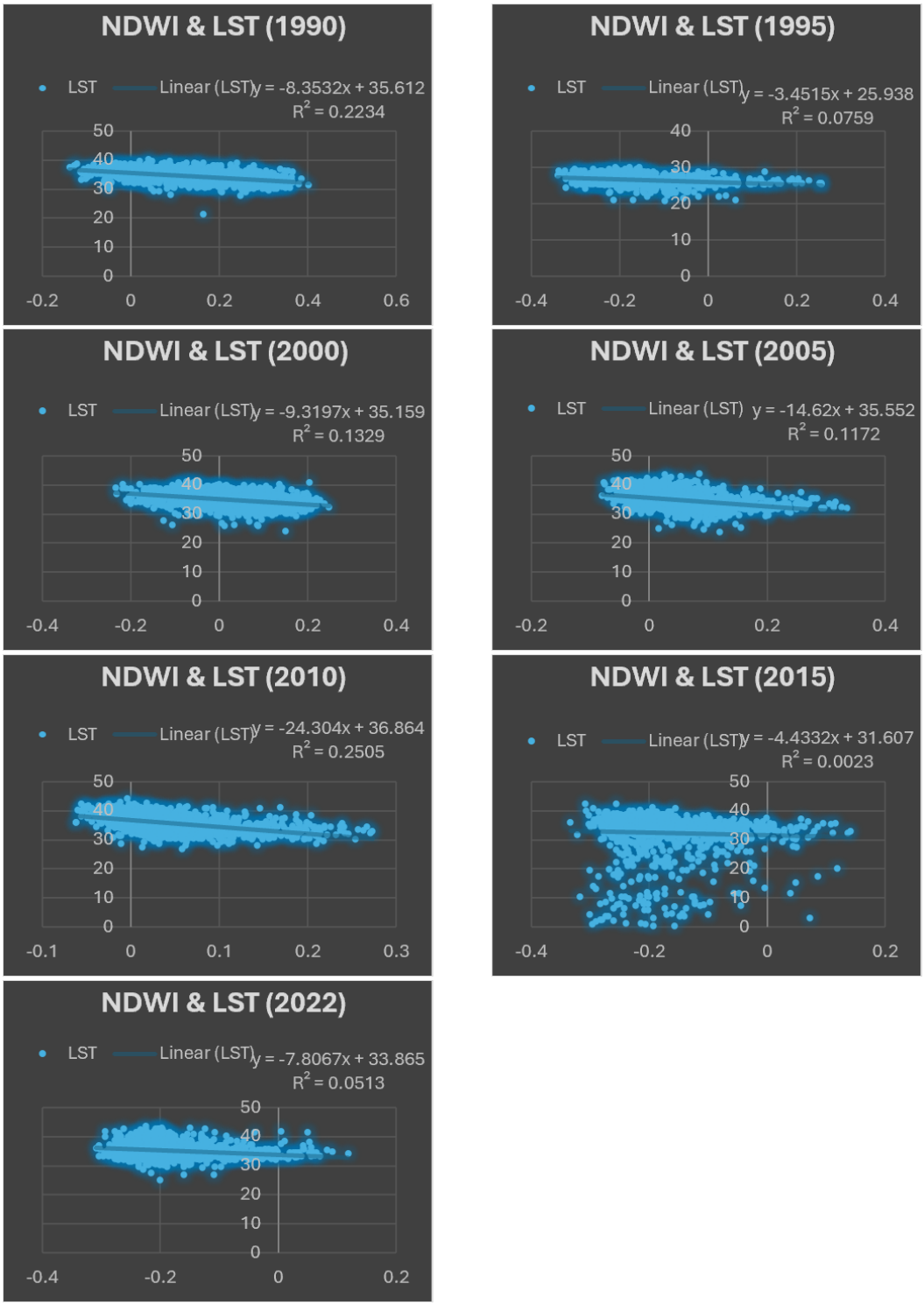

Figure 13: The correlation between NDWI and LST (1990-2022) in the Lahore city.

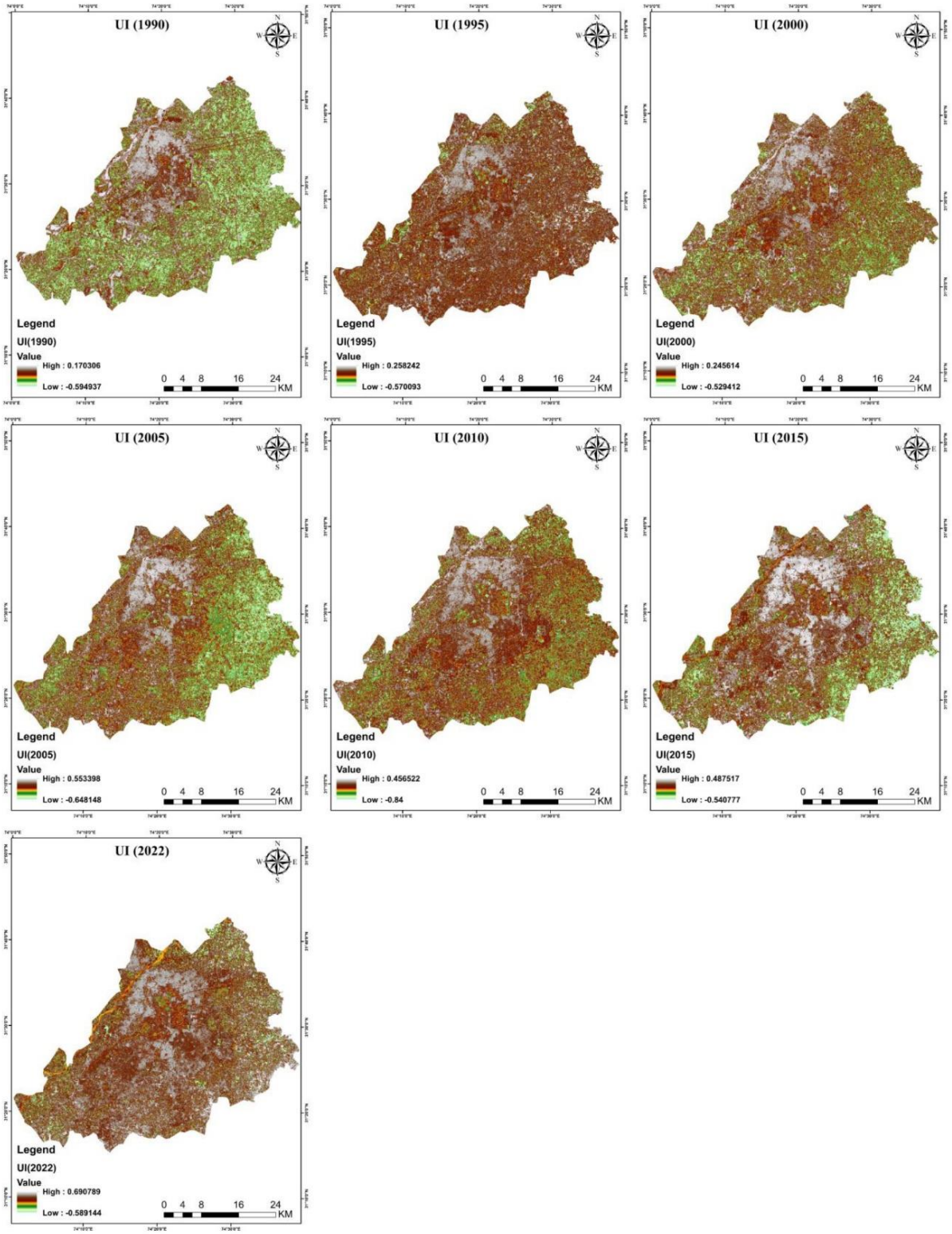

Figure 14: Spatial distribution of UI over Lahore from 1990 to 2022.

Copyright (c) 2026 Author(s)
This work is licensed under a Creative Commons Attribution 4.0 International License.

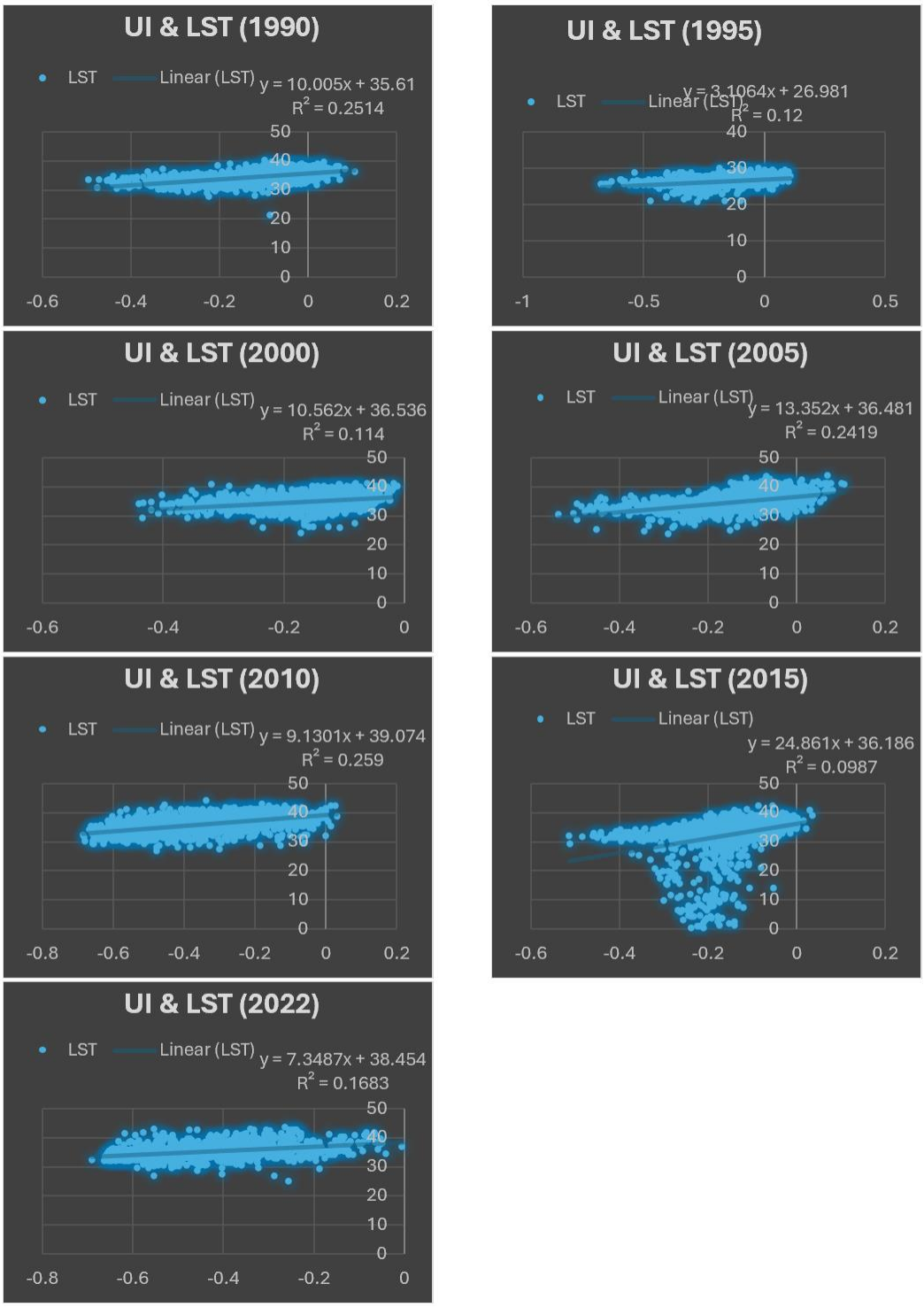

Figure 15: The correlation between UI and LST (1990-2022) in the Lahore city.

Normalized Difference Water Index (NDWI)

The NDWI method is used to measure the amount of liquid water molecules in vegetation that come into contact with sun light. In 1990, 1995, 2000 NDWI values ranged from -0.46 to 0.57, -0.60 to 0.40, -0.40 to 0.61, for the year 2005, 2010; from -0.39 to 0.70, -0.77 to 0.57, for 2015, 2022 -0.42 to 0.38 and - 0.61 to 0.47, respectively, as shown in Figure 12. The correlation between NDWI and LST is strongly positive in 1990, 1995, 2000, the value was 0.86, 0.80, 0.68,

while in 2005, 2010 the value was 0.75, 0.78, the 2015 and 2022 NDWI correlation value was between 0.89 and 0.69 as shown in Figure 13.

The Urban Transformation Index, which quantifies the increase in impermeable regions between 1990 and 2022; -0.59 to 0.17, -0.57 to 0.25, -0.52 to 0.24, -0.64 to 0.55, -0.84 to 0.45, -0.54 to 0.48, and -0.58 to 0.69 respectively, were the ranges of UI values (Figure 14). The numbers gradually increased, indicating that the area beneath waterproof coverings had grown during the previous few decades. There was a considerable positive correlation between UI and LST. For 1990, 1995, 2000, and 2005, the correlation was 0.96, 0.97, 0.97, and 0.98; for 2010, 2015, and 2022, it was 0.98, 0.78, and 0.98 (Figure 15). There is a substantial favorable link between LST and waterproof surfaces. Their relationship is directly proportional. Since water cannot pass through the sealed surfaces and evaporation cannot take place, the temperature rises as the seal strength increases.

DISCUSSION

The results of this study make it clear that Lahore's landscape has changed dramatically over the past three decades, and these changes are closely tied to rising land surface temperatures. There has been a reduction of the vegetation cover that was 71 percent in 1990 to only 45 percent in 2022. This degradation indicates the stress of ever-increasing population, agricultural land conversion, and residential and commercial development. It has also been observed in other rapidly developing South Asian cities, where expansion of built-up areas has been accompanied by the loss of green areas and ecological balances (Athick et al., 2019; Ranagalage et al., 2021). The trend of settlement growth in Lahore is not an exception to the other cities of the world where urbanization is not planned (Javed & Riaz, 2019).

These changes in land cover have been the direct cause of increase in LST. Urban areas that are covered by large building enclosures retain much more heat than green systems do, and due to which thermal hotspots are generated, reinforcing the urban heat island effect. Rise in temperature of Lahore, which grew by an average of 30 ºC in 1990, to over 50 ºC in 2022, is indicative of how diminished evapotranspiration, disappearance of trees and extensive impervious surfaces are changing the thermal profile of the city. Similar increases in LST have been reported in corresponding studies in Islamabad, Faisalabad, and Gilgit because of land conversion and depletion of ecological buffers (Ahmed et al., 2019; Sadiq Khan et al., 2020; Zaman et al., 2020).

The association between NDVI and the LST is negative in all years, emphasizing the role played by vegetation in ensuring the local climatic environments are cooler. Regions of low NDVI were always warmer supporting the cooling effects of evaporative cooling and shading. The present relation is reflected in China, India, and other megacities around the world where urban heating has been aggravated by vegetation loss (Huang et al., 2019; Rahimi et al., 2025).

The positive relationships between LST and NDBI, NDBaI and UI indicate that built-up and barren surfaces are the significant factors that contribute to temperature increase in Lahore. Concrete and asphalt which are impervious absorb heat in the day and dissipate gradually in the night, making warm conditions last much later than daylight. The same thing occurs in barren land due to low moisture level and direct radiation exposure, which is similar to other semi-arid and rapidly urbanizing regions (Mohajerani et al., 2017; Ramzan et al., 2022).

The trends of NDWI also depict a decrease in the moisture supply, an expected trend since urbanization continues to spread to wetlands, agricultural channels, and peri-urban water bodies. The presence of less water undermines natural cooling. Some studies indicate that the cities with similar land changes exhibit the same drying and heating patterns (Majumdar et al., 2023; Ren et al., 2024).

The CA-Markov model also shows a threatening forecast of 2050, which is a loss of vegetation up to 37 percent and settlement growth above 45 percent. With this trend, the city is likely to experience more thermal stress, magnified UHI impacts, and worsening city livability. These estimates are consistent with world estimates which indicate that South Asian megacities are moving toward hazardous climatic levels (Aboulnaga et al., 2024; Lelieveld et al., 2015).

Although the findings strongly prove the effect of LULC change on LST dynamics, some limitations cannot be ignored. Detection of fine-scale urban features and CA-Markov projections are both limited by the fact that they use medium-resolution Landsat imagery and are based on historical transition probabilities respectively. However, the similarity in trends observed with the international case studies of other South Asian and global megacities supports the accuracy of the findings and their applicability in urban climate adaptation planning.

Altogether, the results indicate that the existing pattern of urbanization of Lahore is forcing the city towards becoming more vulnerable to the environment. Further vegetation destruction and augmentation of hard surfaces will probably exacerbate heatwaves, hike energy demand, overloading water resources, and decrease biodiversity. The future may get even more troublesome to handle without timely interventions including urban greening, rehabilitation of degraded aesthetic and landscapes, vertical growth regulation, and climate sensitive planning. The findings can be used to advocate the significance of implementing sustainable land management measures in line with SDG 11 (sustainable cities) and SDG 13 (climate action).

Copyright (c) 2026 Author(s)
This work is licensed under a Creative Commons Attribution 4.0 International License.

CONCLUSION

The study demonstrates that the landscape of Lahore has rapidly changed because of the continued urban growth and expansion and it has significantly contributed to the increase in land surface temperatures. Deforestation and the gradual expansion of urbanization and development have decreased the cooling capability of nature and increased heat retention within the city. It was evident that vegetation had a cooling effect while built-up and barren areas playing a significant role in increasing temperatures.

These results emphasize the necessity of more eco-friendly city planning, rehabilitation of green spaces and policies that allow climate-sensitive development. Otherwise, the environmental issues of the city can increase over the next decades.

HIGHLIGHTS

- Vegetation cover dropped sharply from 71% in 1990 to 45% in 2022.
- Built-up area increased from 13.54% to 36.77% during the same period.
- Land surface temperature rose from around 30°C to more than 50°C between 1990 and 2022.
- NDVI was identified to have a strong negative relationship with LST which validated the cooling effect of vegetation.
- NDBI, NDBaI, and UI exhibited high positive associations with LST, which indicate the presence of impervious and barren surfaces in increasing temperature.
- CA-Markov projections suggest additional vegetation loss (to 37%), and settlement growth (to 45% by 2050).

DECLARATIONS

AI Usage Declaration

In line with COPE guidelines, AI-assisted tools were used only for language editing and formatting and did not contribute to scientific content, data, analysis, or conclusions. All responsibility for the manuscript rests with the authors.

Link with Thesis

It is declared that the manuscript is relevant to a graduation thesis of at least one of the authors. However, the academic repository of their institute is not a formal publishing entity, therefore, they retain the full rights to publish the current article without any formal permission.

REFERENCES

Abdulrahman, A. I., & Ameen, S. A. (2020). Predicting Land use and land cover spatiotemporal changes utilizing CA-Markov model in Duhok district between 1999 and 2033. *Academic Journal of Nawroz University*, *9*(4), 71-80.

Aboulnaga, M., Trombadore, A., Mostafa, M., & Abouaiana, A. (2024). Understanding urban heat Island effect: causes, impacts, factors, and strategies for better livability and climate change mitigation and adaptation. In *Livable Cities: Urban Heat Islands Mitigation for Climate Change Adaptation Through Urban Greening* (pp. 283-366). Springer.

Ahmed, A., ul Hassan, S. N., Baig, S., Khan, M. Z., & Muhammad, A. (2019). The Response of Land Surface Temperature to the Changing Land-Use Land-Cover in a Mountainous Landscape under the Influence of Urbanization: Gilgit City as a case study in the Hindu Kush Himalayan Region of Pakistan: The Response of Land Surface Temperature to the Changing Land-Use Land-Cover in a Mountainous Landscape under the Influence of Urbanization: Gilgit City as a case study in the Hindu Kush Himalayan Region of Pakistan. *International Journal of Economic and Environmental Geology*, *10*(3), 40-49.

Ali, M., Siddique, I., & Abbas, S. (2022). Characterizing air pollution and its association with emission sources in Lahore: A guide to adaptation action plans to control pollution and smog. *Applied Sciences*, *12*(10), 5102.

Athick, A. M. A., Shankar, K., & Naqvi, H. R. (2019). Data on time series analysis of land surface temperature variation in response to vegetation indices in twelve Wereda of Ethiopia using mono window, split window algorithm and spectral radiance model. *Data in brief*, *27*, 104773.

Azizi, P., Soltani, A., Bagheri, F., Sharifi, S., & Mikaeili, M. (2022). An integrated modelling approach to urban growth and land use/cover change. *Land*, *11*(10), 1715.

Demisse Negesse, M., Hishe, S., & Getahun, K. (2024). LULC dynamics and the effects of urban green spaces in cooling and mitigating micro-climate change and urban heat island effects: a case study in Addis Ababa City, Ethiopia. *Journal of Water and Climate Change*, *15*(7), 3033-3055.

Dutta, D., Rahman, A., Paul, S., & Kundu, A. (2019). Changing pattern of urban landscape and its effect on land surface temperature in and around Delhi. *Environmental monitoring and assessment*, *191*(9), 551.

Dutta, D., Rahman, A., Paul, S., & Kundu, A. (2022). Spatial and temporal trends of urban green spaces: An assessment using hyper-temporal NDVI datasets. *Geocarto International*, *37*(25), 7983-8003.

Ekaputri, R., Hidayat, T., Surtikanti, H., & Surakusumah, W. (2024). Modeling vegetation density with remote sensing, normalized difference vegetation index and biodiversity plants in watershed area. *Global Journal of Environmental Science & Management (GJESM)*, *10*(4).

Feng, L., Naz, I., Quddoos, A., Zafar, Z., Gan, M., Aslam, M., Hussain, Z. K., Soufan, W., & Almutairi, K. F. (2025). Exploring rangeland dynamics in Punjab, Pakistan: Integrating LULC, LST, and remote sensing for ecosystem analysis (2000–2020). *Rangeland Ecology & Management*, *98*, 377-388.

Haque, M., & Basak, R. (2017). Land cover change detection using GIS and remote sensing techniques: a spatio-temporal study on Tanguar Haor, Sunamganj, Bangladesh. Egypt J Remote Sens Space Sci 20 (2): 251–263. In.

Huang, K., Li, X., Liu, X., & Seto, K. C. (2019). Projecting global urban land expansion and heat island intensification through 2050. *Environmental Research Letters*, *14*(11), 114037.

Hussain, S., Mubeen, M., Ahmad, A., Majeed, H., Qaisrani, S. A., Hammad, H. M., Amjad, M., Ahmad, I., Fahad, S., & Ahmad, N. (2023). Assessment of land use/land cover changes and its effect on land surface temperature using remote sensing techniques in Southern Punjab, Pakistan. *Environmental Science and Pollution Research*, *30*(44), 99202-99218.

Javed, N., & Riaz, S. (2019). Issues in urban planning and policy: The case study of Lahore, Pakistan. In *New Urban Agenda in Asia-Pacific: Governance for sustainable and inclusive cities* (pp. 117-162). Springer.

Jimenez-Munoz, J. C., Sobrino, J. A., Skoković, D., Mattar, C., & Cristobal, J. (2014). Land surface temperature retrieval methods from Landsat-8 thermal infrared sensor data. *IEEE Geoscience and remote sensing letters*, *11*(10), 1840-1843.

Kaiser, E. A., Rolim, S. B. A., Grondona, A. E. B., Hackmann, C. L., de Marsillac Linn, R., Käfer, P. S., da Rocha, N. S., & Diaz, L. R. (2022). Spatiotemporal influences of LULC changes on land surface temperature in rapid urbanization area by using Landsat-TM and TIRS images. *Atmosphere*, *13*(3), 460.

Karakuş, C. B. (2019). The impact of land use/land cover (LULC) changes on land surface temperature in Sivas City Center and its surroundings and assessment of Urban Heat Island. *Asia-Pacific Journal of Atmospheric Sciences*, *55*(4), 669-684.

Lelieveld, J., Evans, J. S., Fnais, M., Giannadaki, D., & Pozzer, A. (2015). The contribution of outdoor air pollution sources to premature mortality on a global scale. *Nature*, *525*(7569), 367-371.

Liu, J., Hagan, D. F. T., Holmes, T. R., & Liu, Y. (2022). An analysis of spatio-temporal relationship between satellite-based land surface temperature and station-based near-surface air temperature over Brazil. *Remote Sensing*, *14*(17), 4420.

Majumdar, M., Ziaul, S., Pal, S., & Debanshi, S. (2023). Urban effects on hydrological status and trophic state in peri-urban wetland. In *Advancements in urban environmental studies: Application of geospatial technology and artificial intelligence in urban studies* (pp. 179-199). Springer.

Meer, M. S., & Mishra, A. K. (2020). Land use/land cover changes over a district in northern India using remote sensing and GIS and their impact on society and environment. *Journal of the Geological Society of India*, *95*(2), 179-182.

Mir, Y. H., Mir, S., Ganie, M. A., Bhat, J. A., Shah, A. M., Mushtaq, M., & Irshad, I. (2025). Overview of land use and land cover change and its impacts on natural resources. In *Ecologically Mediated Development: Promoting Biodiversity Conservation and Food Security* (pp. 101-130). Springer.

Mohajerani, A., Bakaric, J., & Jeffrey-Bailey, T. (2017). The urban heat island effect, its causes, and mitigation, with reference to the thermal properties of asphalt concrete. *Journal of environmental management*, *197*, 522-538.

Mumtaz, F., Tao, Y., De Leeuw, G., Zhao, L., Fan, C., Elnashar, A., Bashir, B., Wang, G., Li, L., & Naeem, S. (2020). Modeling spatio-temporal land transformation and its associated impacts on land surface temperature (LST). *Remote Sensing*, *12*(18), 2987.

Negesse, M. D., Hishe, S., & Getahun, K. (2024). Urban land use, land cover change and urban microclimate dynamics in Addis Ababa, Ethiopia. *Discover Environment*, *2*(1), 71.

Qureshi, H. U., Shah, S. M. H., & Teo, F. Y. (2023). Trend assessment of changing climate patterns over the major agro-climatic zones of Sindh and Punjab. *Frontiers in Water*, *5*, 1194540.

Rafiq, M., Mishra, A. K., & Meer, M. S. (2018). On land-use and land-cover changes over Lidder Valley in changing environment. *Annals of GIS*, *24*(4), 275-285.

Rahimi, E., Dong, P., & Jung, C. (2025). Global NDVI-LST correlation: Temporal and spatial patterns from 2000 to 2024. *Environments*, *12*(2), 67.

Ramzan, M., Saqib, Z. A., Hussain, E., Khan, J. A., Nazir, A., Dasti, M. Y. S., Ali, S., & Niazi, N. K. (2022). Remote sensing-based prediction of temporal changes in land surface temperature and land use-land cover (LULC) in urban environments. *Land*, *11*(9), 1610.

Ranagalage, M., Morimoto, T., Simwanda, M., & Murayama, Y. (2021). Spatial analysis of urbanization patterns in four rapidly growing south Asian cities using Sentinel-2 Data. *Remote Sensing*, *13*(8), 1531.

Rees, G., Hebryn-Baidy, L., & Belenok, V. (2024). Temporal variations in land surface temperature within an urban ecosystem: A comprehensive assessment of land use and land cover change in Kharkiv, Ukraine. *Remote Sensing*, *16*(9), 1637.

Ren, Z., Wang, C., Guo, Y., Hong, S., Zhang, P., Ma, Z., Hong, W., Wang, X., Geng, R., & Meng, F. (2024). The cooling capacity of urban vegetation and its driving force under extreme hot weather: A comparative study between dry-hot and humid-hot cities. *Building and Environment*, *263*, 111901.

Robinson, N. P., Allred, B. W., Jones, M. O., Moreno, A., Kimball, J. S., Naugle, D. E., Erickson, T. A., & Richardson, A. D. (2017). A dynamic Landsat derived normalized difference vegetation index (NDVI) product for the conterminous United States. *Remote Sensing*, *9*(8), 863.

Sadiq Khan, M., Ullah, S., Sun, T., Rehman, A. U., & Chen, L. (2020). Land-use/land-cover changes and its contribution to urban heat Island: A case study of Islamabad, Pakistan. *Sustainability*, *12*(9), 3861.

Shahid, I., & Venturi, L. A. B. (2025). Spatial Analysis of Land Use/Land Cover Changes in Mardan, Pakistan: A Decadal Study Using GIS and Remote Sensing. *Social Science Review Archives*, *3*(3), 944-954.

Shiflett, S. A., Liang, L. L., Crum, S. M., Feyisa, G. L., Wang, J., & Jenerette, G. D. (2017). Variation in the urban vegetation, surface temperature, air temperature nexus. *Science of the Total Environment*, *579*, 495-505.

Siddique, M. A., Dongyun, L., Li, P., Rasool, U., Khan, T. U., Farooqi, T. J. A., Wang, L., Fan, B., & Rasool, M. A. (2020). Assessment and simulation of land use and land cover change impacts on the land surface temperature of Chaoyang District in Beijing, China. *PeerJ*, *8*, e9115.

Singh, K. V., Setia, R., Sahoo, S., Prasad, A., & Pateriya, B. (2015). Evaluation of NDWI and MNDWI for assessment of waterlogging by integrating digital elevation model and groundwater level. *Geocarto International*, *30*(6), 650-661.

Singh, S., Priyadarshni, P., & Pandey, P. (2023). Impact of urban heat island: a local-level urban climate phenomenon on urban ecology and human health. In *Advanced Remote*

Copyright (c) 2026 Author(s)
This work is licensed under a Creative Commons Attribution 4.0 International License.

Sensing for Urban and Landscape Ecology (pp. 113-128). Springer.

Tan, J., Yu, D., Li, Q., Tan, X., & Zhou, W. (2020). Spatial relationship between land-use/land-cover change and land surface temperature in the Dongting Lake area, China. *Scientific Reports*, *10*(1), 9245.

Tarasov, A. V., & Rakhmanov, R. S. (2023). Climatic Norms, Definition Periods: Methods for Determining the Areas of Biological Comfort/Discomfort. In *Marine Climate of Russian Coastal Territories: Public Health Aspects of Biological Adaption* (pp. 19-36). Springer.

Tariq, A., & Shu, H. (2020). CA-Markov chain analysis of seasonal land surface temperature and land use land cover change using optical multi-temporal satellite data of Faisalabad, Pakistan. *Remote Sensing*, *12*(20), 3402.

Teimouri, R., & Karbasi, P. (2024). Analyzing the contribution of urban land uses to the formation of urban heat islands in Urmia city. *Urban Science*, *8*(4), 208.

Traore, M., Lee, M. S., Rasul, A., & Balew, A. (2021). Assessment of land use/land cover changes and their impacts on land surface temperature in Bangui (the capital of Central African Republic). *Environmental Challenges*, *4*, 100114.

Ullah, W., Ahmad, K., Ullah, S., Tahir, A. A., Javed, M. F., Nazir, A., Abbasi, A. M., Aziz, M., & Mohamed, A. (2023). Analysis of the relationship among land surface temperature (LST), land use land cover (LULC), and normalized difference vegetation index (NDVI) with topographic elements in the lower Himalayan region. *Heliyon*, *9*(2).

Wu, D., Liu, J., Wang, S., & Wang, R. (2010). Simulating urban expansion by coupling a stochastic cellular automata model and socioeconomic indicators. *Stochastic Environmental Research and Risk Assessment*, *24*(2), 235-245.

Yasin, M. Y., Abdullah, J., Noor, N. M., Yusoff, M. M., & Noor, N. M. (2022). Landsat observation of urban growth and land use change using NDVI and NDBI analysis. IOP Conference Series: Earth and Environmental Science,

Zaman, H. M., Saqib, Z., Bokhari, A. S., Akhtar, N., & Amir, S. (2020). The dynamics of urbanizations and concomitant land use land cover transformations in planned and quasi-planned urban settlements of Pakistan. *Geography, Environment, Sustainability*, *13*(4), 107-120.

Zhang, T., Huang, X., Wen, D., & Li, J. (2017). Urban building density estimation from high-resolution imagery using multiple features and support vector regression. *IEEE Journal of Selected Topics in Applied Earth Observations and Remote Sensing*, *10*(7), 3265-3280.

Zhao, X., & Miao, C. (2022). Spatial-temporal changes and simulation of land use in metropolitan areas: a case of the zhengzhou metropolitan area, China. *International Journal of Environmental Research and Public Health*, *19*(21), 14089.

Zheng, Y., Tang, L., & Wang, H. (2021). An improved approach for monitoring urban built-up areas by combining NPP-VIIRS nighttime light, NDVI, NDWI, and NDBI. *Journal of cleaner production*, *328*, 129488.